Evolution of the Corrosion-inhibiting Efficiency of Novel Hydrazine Derivatives against Corrosion of Stainless Steel 201 in Acidic Medium

A. S. Fouda[1,], S. A. Abd El-Maksoud[2], A. El-Hossiany[3], A. Ibrahim[1]*

[1] Department of Chemistry, Faculty of Science, El-Mansoura University, El-Mansoura-35516, Egypt,
[2] Department of Chemistry, Faculty of Science, Port Said University, Port Said, Egypt.
[3] Delta Fertilizers Company in Talkha, Egypt
[*]E-mail: asfouda@hotmail.com

The corrosion inhibition effectiveness of some hydrazine derivatives (HD) as corrosion inhibitors for stainless steel (SS 201) in 1.0 M HCl had confirmed using chemical and electrochemical methods. The studies were achieve at various temperatures (25-45°C). The thermodynamic parameters were determined. HD have been found to be more effective corrosion inhibitors at lower temperatures. Adsorption isotherm was determined and was found to follow Langmuir's adsorption isotherm. Inhibition efficiencies at different HD concentrations were determined using chemical and electrochemical techniques. Polarization data revealed that these HD act as mixed-kind inhibitors. Morphology of the surface was examined utilizing Fourier transform infrared (FTIR) and atomic force microscopy (AFM). The obtained inhibition efficiency from different techniques were in a high agreement, confirming the validity of the used all techniques for stainless steel corrosion in hydrochloric acid medium.

1. INTRODUCTION

Corrosion is a severe problem facing the world industrial projects, arising because of material interactions with the environment [1]. The most effective and practical method to decrease corrosion processes is the addition of inhibitor to the metal's environment [2]. Inhibitors are compounds that suppress the rate of corrosion of metals by adsorbing on the surface of the metals either through physical or chemical adsorption and thereby, change the structure of electrical double layer [3, 4]. The search for new and efficient corrosion inhibitors requires the clarification of interactions between

inhibitor molecules and metal surfaces. In this concern, organic compounds corrosion inhibitors have been assumed to be suitable as ecofriendly in inhibiting severe corrosion attack which caused due to hetro atom existence with the metal surface, hence, retarding the redox reactions that takes place, as it shown greater inhibition that linked to the presence of electron donor atoms (heteroatoms) such as N,S,O,….etc that containing lone pair of electrons or containing other clouds of Л electrons in aromatic rings, long carbon chain length as well as triple bond in their molecular structures that shared with the active sites on the SS 201 surface during these redox reactions [5, 6]

Organic compounds are outstanding for their productivities as corrosion protection and those including "N" have frequently mentioned to in the literature [7-9], imines [10], dioxan-water mixtures [11], quaternary ammonium, salts based on 2-acetylallylchloride [12], 2-mercapto benzimidazole [13], Ethoxylated fatty alcohols[14], Schiff base compounds [15], pyrrole and its derivatives [16], Pyrazolo carbothioamide [17], 1,3-Thiazolidin-5-one [18], Pyrazolone [19], Distyryl [20]. The current study reports the performance of HD. The objective of this study is to examine the inhibiting behavior of some hydrazine derivatives on the corrosion of SS 201 in 1.0M HCl utilizing chemical and electrochemical tests. The surface morphology of SS 201was also analyzed.
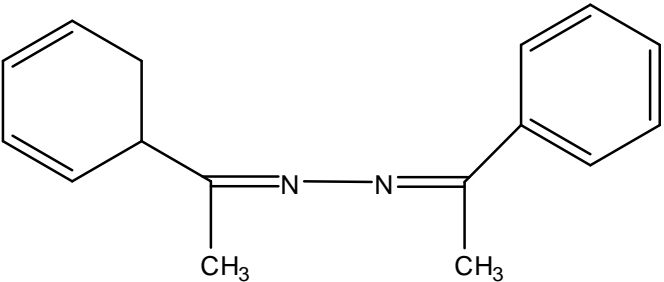
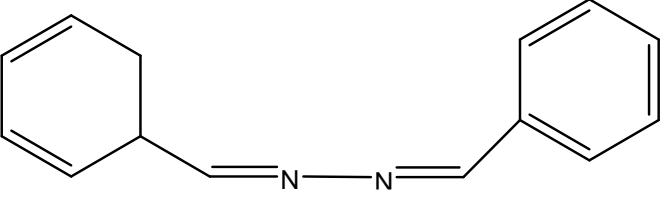## 2. MATERIALS AND TECHNIQUES

2.1 Materials and Solutions

The metal sample conformation in weight % is: Si 1, C 0.15, Cr 16-18, Ni 3.5-5.5, N 0.25, S 0.03, P 0.06, Mn 5.5-7.5 and Fe the rest

2.2 Inhibitor

The inhibitors were prepared in the research laboratory according to an earlier designated investigation method, characterization of these inhibitors was done using, NMR, IR spectra and elemental analysis. The structural formula of the studied inhibitors is recorded in Table 1.

Table 1. Chemical assemblies of the studied organic compounds

Inhibitor	Structures, Names	Mol. Formulas, Mol. Weights
A	1-(1-(cyclohexa-2,4-dienyl)ethylidene)-2-(1-phenylethylidene)hydrazine	$C_{16}H_{18}N_2$ 238.33

B		$C_{14}H_{14}N_2$ 210.27
	1-benzylidene-2-(cyclohexa-2,4-dienylmethylene)hydrazine	

2.3. Chemicals and Solutions

SS 201 specimens were used. The corrosive solution used is HCl 37%. Solutions of 1.0 M HCl were prepared by dilution with distilled water. The HD stock solution 10^{-3} M was used to prepare (1 $\times 10^{-6}$ - 21 $\times 10^{-6}$ M).The HD inhibitors that used as a part of this research have listed in Table1.

2.4. Methods

2.4.1. Mass Loss (ML) Technique

For ML measurements, the metal coupons were cut into ($2\times2\times0.2$ cm) x 2 pieces, and were polished utilizing various grades of emery papers up to 1200 grit size. The pieces were cleaned by acetone and bidistilled water, dried utilizing filter papers, and then weighed. Seven pieces of SS 201 were hanging in test solutions without and with organic compounds utilizing suitable glass hooks. After definite interval time, the pieces were taken out from the solutions, rinsed, dried, and weighed again. The ML for each piece was then taken. The % IE of HD and surface coverage of SS 201 (θ) from ML tests were determined utilizing the next equation:

$$\% \ IE = \theta \ x \ 100 = [(W^o − W)\diagup W^o] \times 100 \tag{1}$$

Where W is the ML of the metal with HD and W^o is the ML of the metal without HD.

2.4.2 Potentiodynamic Polarization (PP) Technique

(PP) is a useful method because it gives more information about the corrosion mechanism and the factors affecting the corrosion process and inhibition behavior of the inhibitors. This is done by measuring the potential- current characteristics of the metal/ solution system. The potential range was (-1.0 to - 0.6V vs. SCE) at OCP with a scan rate 1 mVs^{-1}.

2.4.3. EIS Tests

This technique was done by AC signs of 5 mV peak to peak amplitude and at frequency range of 10^5 Hz to 0.1 Hz. The (% IE) and θ were founded from eq. (2) [23]:

$$\% \ IE = 100 \ x \ \theta = 100 \ x \ [(\ R_{ct} − R^°_{ct} \ )\diagup R_{ct}] \tag{2}$$

Where $R^°_{ct}$ is the charge transfer resistance with HD and R_c is the charge transfer resistance without HD

2.4.4. EFM Tests

This technique used two frequencies of range 2 and 5 Hz depended on three conditions [24]. The (i_{corr}), (β_c and β_a) and (CF-2, CF-3) (Causality factors) were measure by the greater two peaks [25].

The electrochemical techniques have been performed using PCI4-G750 Potentiostat/Galvanostat and a personal computer with Gamry PCI4-G750 software for calculations. The used electrical circuit consists of three electrodes (SCE reference electrode, Pt auxiliary electrode and SS 201 electrode). 1 cm^2 of the SS 201 electrode is prepared, and cleaned as illustrated in ML method. The pre-immersion oxide film was reduced by given a time period of about 20 minutes for open circuit potential (OCP). All electrochemical studies were performed at 25 ±1 °C.

2.4.5. Surface Examinations

SS 201 pieces were dipped in testing solutions for one day. Then, they were polished, dried and analyzed by (FTIR) and (AFM).

3. RESULTS AND DISCUSSION

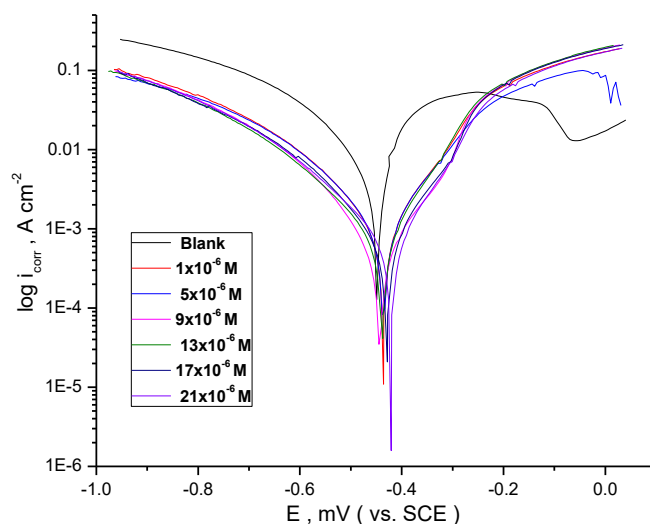*3.1. Potentiodynamic Polarization (PP) Tests*

Figure 1. PP curves of the SS 201 dissolution in 1.0M HCl with and without different concentrations of compound (A) at 25°C

Tafel curves of SS 201 electrode in 1.0 M HCl with and without various contents of compound (A) can be studied from Figure 1. Similar curves were received for other compound (B) (not displayed). Table 2 shows the determined values of $i_{corr.}$, $E_{corr.}$, Tafel slopes (β_a and β_c), k_{corr}, θ and %IE, from Table 2 the presence of these compounds have effect on both of cathodic and anodic processes and the IE rises with rise of the HD content. E_{corr} was a little changed, indicating that HD act

as a mixed–kind inhibitor. i_{corr} reduced through the HD addition to the corrosive solution. % IE and (θ) were found from eq. (3):

$$\% \text{ IE} = \theta \times 100 = [(i_{corr} - i_{corr(inh)}) / i_{corr}] \times 100 \tag{3}$$

Where, i_{corr} is the current density in absence of HD and i_{corr} in presence of HD. The order of HD according to % IE is being: A > B.

Table 2. PP parameters (i_{corr}, E_{corr}, β_c, β_a, k_{corr}, θ, and % IE) of SS 201 dissolution in 1.0M HCl with and without different concentrations of HD at 25°C

Comp	*Conc.,* $x10^6$ *M*	i_{corr}, μA cm^{-2}	- E_{corr}, mV vs SCE	β_a mV dec^{-1}	β_c mV dec^{-1}	C.R mpy	θ	*% IE*
Blank	0.0	5310	448	120	152	25.4		
A	1	1630	456	103	157	23.2	0.693	69.3
	5	1358	469	112	165	22.1	0.744	74.4
	9	1151	455	116	145	21.5	0.783	78.3
	13	929	459	95	140	18.9	0.825	82.5
	17	822	461	90	137	16.9	0.845	84.5
	21	726	468	88	155	13.9	0.863	86.3
B	1	1710	465	120	142	23.9	0.678	67.8
	5	1450	471	121	139	23.1	0.727	72.7
	9	1341	451	116	142	22.8	0.747	74.7
	13	1020	456	105	138	20.5	0.808	80.8
	17	992	459	95	139	18.8	0.813	81.3
	21	854	483	97	125	15.3	0.839	83.9

3.2 (EIS) Tests

From Figure 2 the semi-circle diameter had raised by increasing of compound (A) concentration.

Figure 3 indicates the utilizing circuit for fitting the obtained results [26]. Similar curves were received for other compound (not displayed). The C_{dl} and Y^0 were founded from eq. (4) [27]:

$$C_{dl} = Y^0 \omega^{n-1} / \sin [n (\pi/2)] \tag{4}$$

where $\omega = 2\pi f_{max}$, f_{max} is the greater frequency and n is the exponential. R_{ct} increases with the rise of the double layer thickness [28]. From Table 3, the C_{dl} decline as a result of the replacement of adsorbed water molecules by HD species [29]. The order of organic compounds according to % IE is being: A > B.
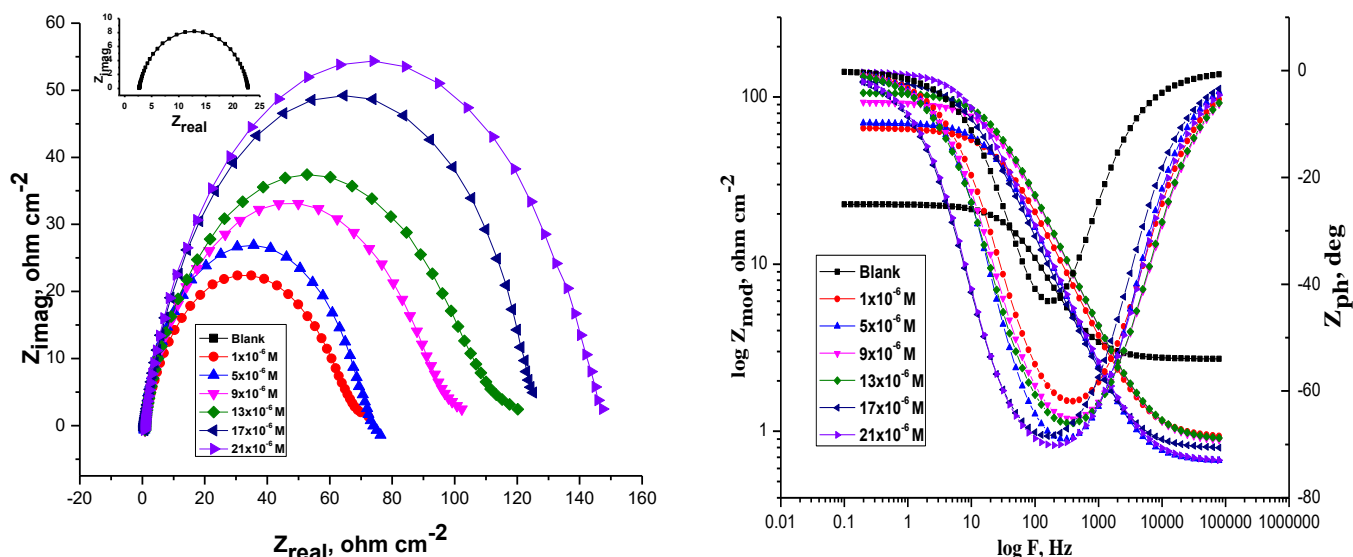
Figure 2. EIS Bode and Nyquist curves for SS 201 in 1.0 M HCl with and without several concentrations of compound (A) 25°C
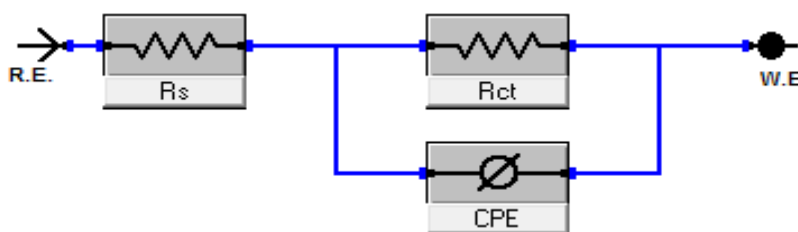

Figure 3. Circuit utilized for fitting the EIS data in 1.0 M HCl

Table 3. EIS parameters for SS 201 in 1.0 M HCl without and with different concentrations of HD at 25°C

Comp	Conc., x 10^6 M	R_{ct}, $\Omega\ cm^2$	C_{dl}, μFcm^{-2}	θ	%IE
Blank	0	23	393		
A	1	72	148	0.681	68.1
	5	79	142	0.709	70.9
	9	98	133	0.765	76.5
	13	118	128	0.805	80.5
	17	128	120	0.820	82.0
	21	155	115	0.852	85.2
B	1	68	158	0.662	66.2
	5	73	151	0.685	68.5
	9	90	145	0.744	74.4
	13	111	138	0.793	79.3
	17	122	124	0.811	81.1
	21	138	120	0.833	83.3

3.3. (EFM) Tests

    EFM is characterized by speed and greatly accuracy in calculating the current data [30]. Figure 4 indicates the EFM of SS 201 in 1.0 M HCl solution and various concentration of HD. The EFM parameters such as (CF-2 and CF-3), (β_c and β_a) and (i_{corr}) can be measured from the higher current peaks. Similar curves were received for other compounds (not displayed). The CF is closer to the standard data proved the validity of the calculated data. The IE% increase with the raising of organic compounds concentrations. The order of HD according to % IE is being: A > B.
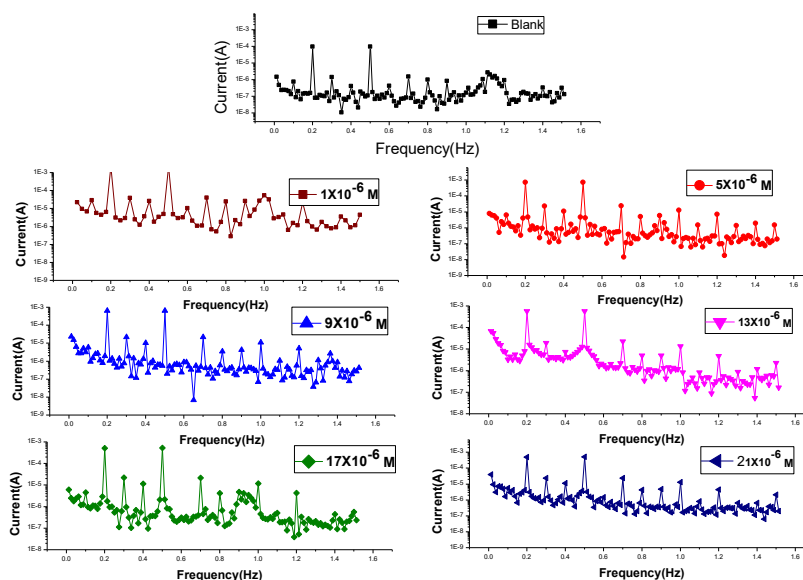

Figure 4. EFM specra for SS 201 in 1.0 M HCl without and with of various concentrations of compound (A) at 25°C

Table 4. EFM parameters for SS 201 in 1.0 M HCl without and with various HD concentrations at 25°C

Comp	Conc., x 10^6 M	i_{corr}, μ A cm^{-2}	β_a, mVdec^{-1}	β_c, mVdec^{-1}	C.R , mpy	CF-2	CF-3	θ	% IE
Blank	0.0	3788	103.2	116.0	173	2.1	3.1	------	-----
A	1	994	106	120	158	2.3	2.9	0.738	73.8
	5	937	99	122	154	1.9	3.0	0.753	75.3
	9	735	88	118	148	1,8	2.8	0.806	80.6
	13	698	87	115	142	2.0	3.1	0.816	81.6
	17	615	98	120	137	1.8	3.0	0.838	83.8
	21	530	96	122	128	2.1	2.9	0.860	86.0
B	1	1115	88	127	161	1.9	3.0	0.706	70.6
	5	985	98	131	158	1.8	29	0.740	74.0
	9	810	96	128	151	1.9	2.8	0.786	78.6
	13	723	85	126	148	2.2	2.8	0.809	80.9
	17	697	88	119	141	2.0	2.7	0.816	81.6
	21	585	92	118	134	1.9	3.1	0.846	84.6

3.4. Mass Loss (ML) Tests

The loss in mass of SS 201 can be studied in the presence of HD at 25°C. Figure 5 shows that the presence of HD decreases the mass loss and therefore corrosion rate. The (%IE) and then θ, of the HD for the SS 201 were founded by eq. (1) [31]. Similar curves were received for other compound (not displayed). The values of %IE are given in Table 5. The order of HD according to % IE is being: A > B.
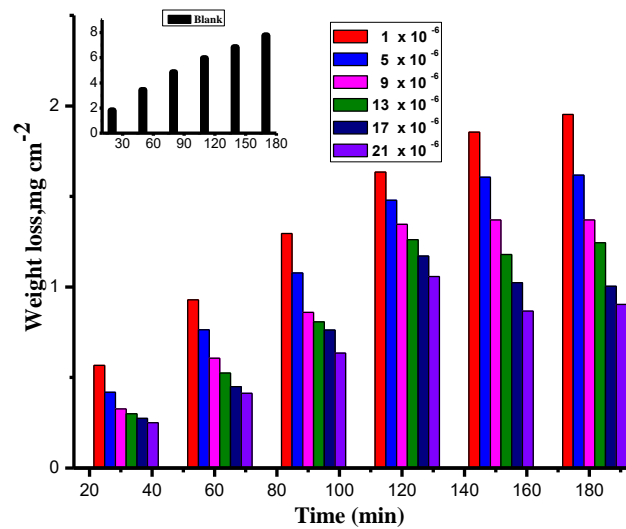

Figure 5. ML-time curves for the corrosion of SS 201 in 1.0 M HCl without and with various concentrations of compound (A) at 25°C

Table 5. CR and %IE of SS 201 in 1.0 M HCl in absence and presence of various concentrations of studied HD after 120 min immersion at 25°C

Organic compounds	A		B	
Conc., x 10^6 M	Θ	% IE	Θ	% IE
1	0.726	72.6	0.714	71.4
5	0.753	75.3	0.744	74.4
9	0.775	77.5	0.767	76.7
13	0.789	78.9	0.782	78.2
17	0.819	81.9	0.797	79.7
21	0.843	84.3	0.815	81.5

3.5 Influence of Temperature

The temperature effect on SS 201 dissolution in corrosive solution without and with different HD concentrations has been studied in temperature range (25-45°C) by ML, as illustrated in Figure 6. The Figure showed that the ML increases with raising the temperature at all HD concentrations. This may referred to molecules desorption from the metal surface at higher temperatures. Increasing of ML with temperature rising is suggestive of physical adsorption. Figure 6 shows %IE against concentration of compound (A) at different temperatures. As shown, %IE decreases with raising temperature at all HD concentrations. Table 6 shows the temperature effect on corrosion rate (CR), θ, and %IE of SS 201.
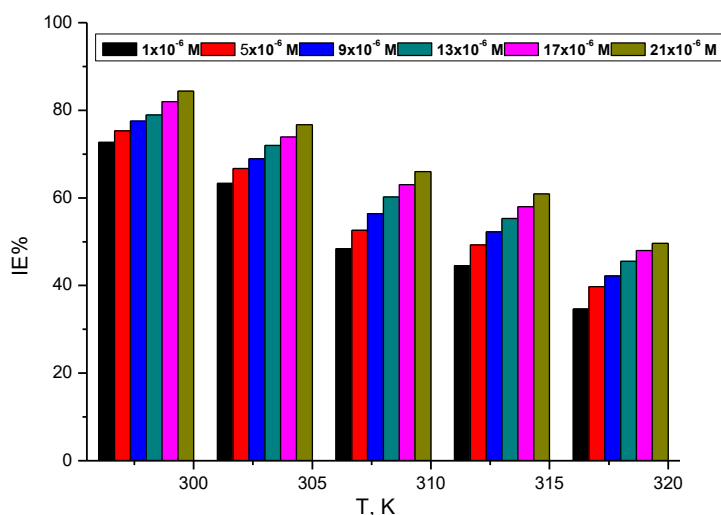

Figure 6. The relationship between % IE and temperature at many concentrations of compound (A) for SS 201 corrosion in 1.0 M HCl

Table 6. Data of % IE, (θ) and (k_{corr}) for SS 201 corrosion after 120 min immersion in 1M HCl before and after addition of various concentrations of compound (A) at various temperatures

Temp.	Conc. [x10^{6}M]	Weight loss mg cm^{-2}	k_{corr} mg cm^{-2} min^{-1}	%IE
	Blank	5.99	4.99	--
	1	1.63	1.36	72.6
	5	1.47	1.23	75.3
25	9	1.34	1.12	77.5
	13	1.26	1.05	78.9
	17	1.085	0.90	81.9
	21	0.937	0.78	84.3
	Blank	7.50	6.25	--
	1	2.75	2.29	63.3
	5	2.49	2.08	66.7
30	9	2.33	1.94	68.9
	13	2.10	1.75	71.9
	17	1.95	1.63	73.9
	21	1.74	1.46	76.7

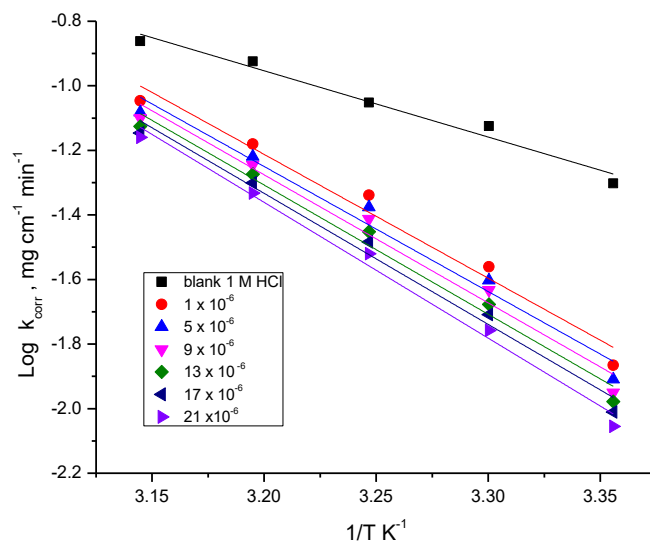|				
	Blank	8.91	7.43	--
	1	4.61	3.83	48.3
	5	4.23	3.52	52.5
35	9	3.89	3.24	56.4
	13	3.54	2.95	60.2
	17	3.29	2.75	63.0
	21	3.03	2.53	66.0
	Blank	11.91	9.93	--
	1	6.61	5.51	44.5
	5	6.04	5.04	49.2
40	9	5.69	4.74	52.2
	13	5.32	4.44	55.3
	17	5.01	4.17	58.0
	21	4.66	3.88	60.9
	Blank	13.74	11.45	--
	1	8.98	7.48	34.6
	5	8.27	6.90	39.7
45	9	7.94	6.62	42.2
	13	7.48	6.24	45.5
	17	7.15	5.96	47.9
	21	6.92	5.77	49.6

Figure 7. Log k_{corr} vs reciprocal of temperature plot for SS 201 in 1.0 M HCl without and with various concentrations of compound (A)

The equation of Arrhenius (6) can be used to measure the activation energy (E^*_a) of the activated complex [32]:

$$C.R. = A \exp (-E^*_a / RT) \qquad (5)$$

where E^*_a is activation energy and T is the absolute temperature. Using Figure 7, E^*_a can be measured (Table 7). Similar curves were received for other compounds (not displayed). E^*_a values

prove that the higher extents of HD impede corrosion effectively by raising the energy barrier of the activated complex and improve that the process is controlled by diffusion [33].

   $(\Delta H^*, \Delta S^*)$ are measured by eq. (7) [34]:

   $C.R. = RT/Nh \exp(\Delta S^*/R) \exp(-\Delta H^*/RT)$ (6)

   Figure 7 shows the relation between $\log (C.R. /T)$ and $(1/T)$ which used to measure the values of ΔH^* and ΔS^* (Table 7).

   The rise in the (ΔH^*) with the presence of the HD reflects the rise in the energy barrier of the corrosion process [35]. The negative values of ΔS^* shows that during the rate-determining step in the formation of activated complex is highly associated than dissociated [36].
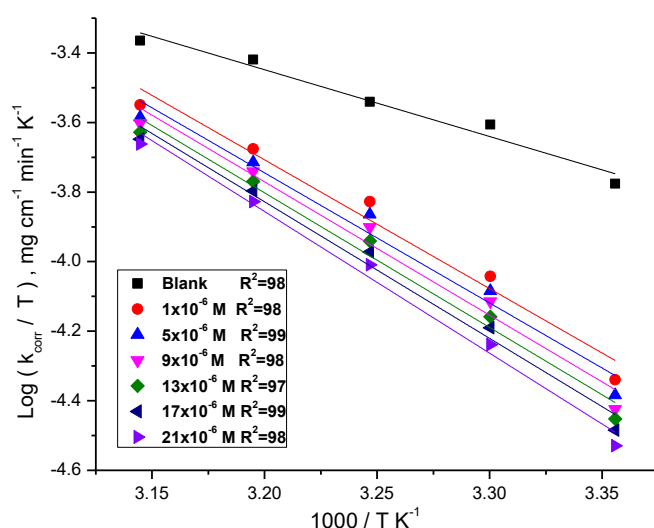

Figure 8. The relation between (log C.R. / T) and 1/ T diagrams for the SS 201 in 1.0 M HCl without and with different concentrations of compound (A)

Table 7. Activation parameters for SS 201 in 1.0 M HCl without and with various concentrations of HD

Comp	Conc., x 10^6 M	E_a^*, kJ mol^{-1}	ΔH^*, kJ mol^{-1}	$-\Delta S^*$, J mol^{-1}K^{-1}
Blank	0.0	33.4	13.4	166.1
A	1	68.5	25.3	56.8
	5	70.8	26.9	52.9
	9	72.9	28.3	50.1
	13	74.6	30.9	45.3
	17	77.7	31.8	30.3
	21	80.5	32.7	21.8
B	1	65.1	24.6	58.4
	5	68.1	25.1	54.7
	9	70.9	27.8	52.1
	13	72.5	29.1	46.4
	17	75.7	30.6	36.0
	21	79.2	31.7	28.6

3.7. Adsorption Isotherms

Figure 9 represented the Langmuir isotherm, which used to calculate Ө values for compound (A). Similar curves were received for other compound (B) (not displayed).The Langmuir equation represented as follows [37].

$$C/Ө = 1/K_{ads} + C \qquad (7)$$

Where K_{ads} is the adsorption constant and C is the HD concentration (M). The ΔG°_{ads} and K_{ads} data are in Table 8. The ΔG^{o}_{ads} founded by**:**

$$\Delta G^{o}_{ads} = - RT \ln (55.5\ K_{ads}) \qquad (8)$$

The HD adsorption is spontaneous and this is proven by the ΔG°_{ads} negative sign. From the data of ΔG^{o}_{ads} (around to -20 kJ mol^{-1}), proven that the HD adsorption is physisorption [38].

Vant't Hoff equation can be used to measure ΔH°_{ads} and ΔS°_{ads} [39] expressed by:

$$\text{Ln K}_{ads} = \frac{-\Delta H^{\circ}_{ads}}{RT} + const \qquad (9)$$

And eq. (10):

$$\Delta G^{o}_{ads} = \Delta H^{o}_{ads} - T\ \Delta S^{o}_{ads} \qquad (10)$$

Figure 10 shows the relation between ΔG^{o}_{ads} and T. A negative sign of ΔS°_{ads} proved that the disorder of corrosion process is decreases by using HD (Table 8) [40].
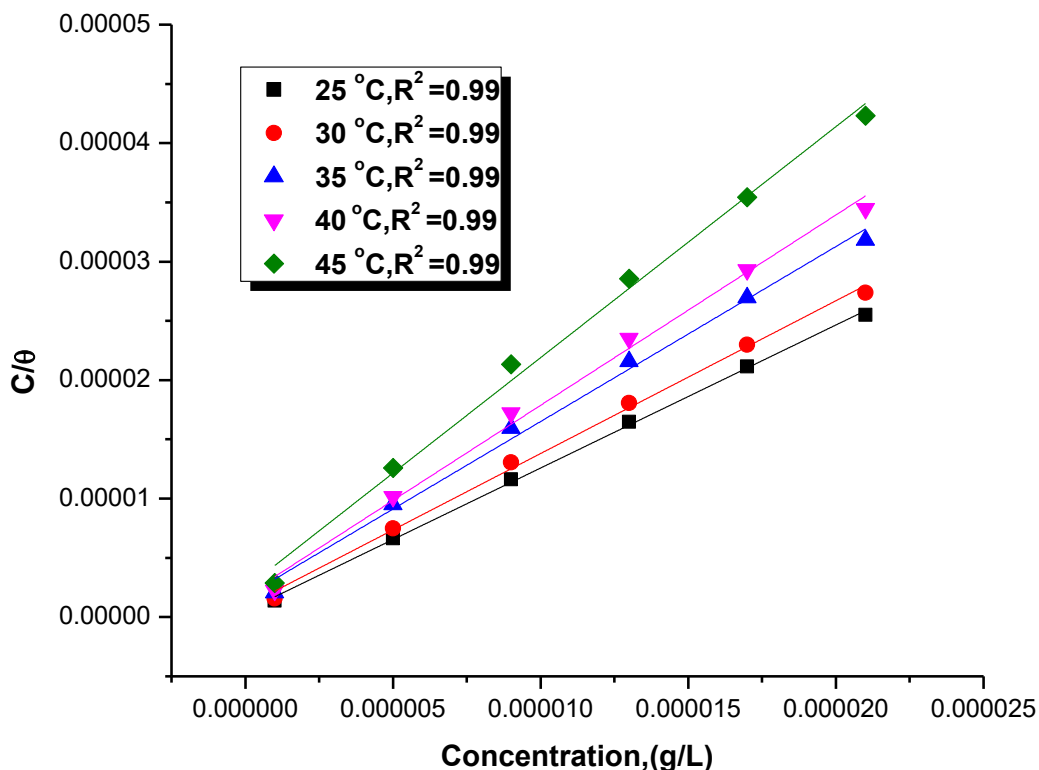

Figure 9. Langmuir isotherm for the compound (A) on SS 201 in 1.0 M HCl
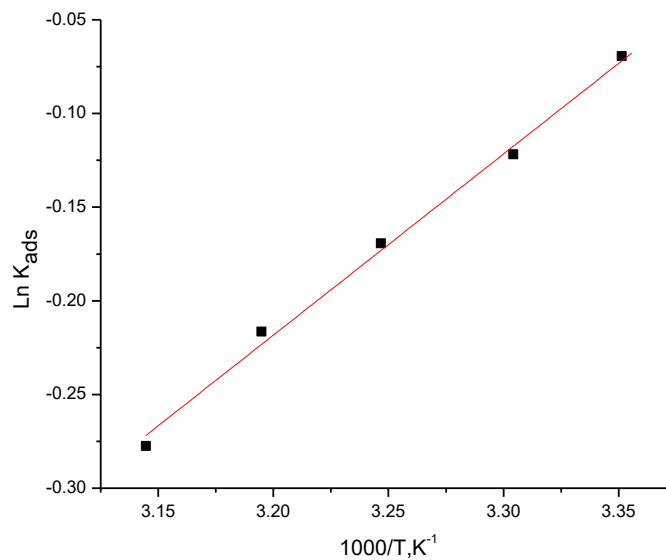
Figure 10. Variation of Ln K_{ads} vs 1/T from Langmuir for the adsorption of compound (A) in 1M HCl

Table 8. Langmuir data for SS 201 in 1.0 M HCl without and with various concentrations of HD at (25°C- 45°C)

| Comp	Temp., K	$-\Delta G^{\circ}_{ads}$ kJ mol^{-1}	$-\Delta H^{\circ}_{ads}$ kJ mol^{-1}	$-\Delta S^{\circ}_{ads}$ J mol^{-}K^{-1}
A	298	20.1		75
	303	19.9		71
	308	19.7	38.5	65
	313	19.2		63
	318	18.8		61
B	298	19.8		73
	303	19.4		69
	308	18.8	29.4	63
	313	18.4		61
	318	18.3		60

3.8. (AFM) analysis

AFM is a remarkable technique used for measuring the surface roughness with high resolution [41]. Many details about SS 201 surface morphology can be obtained from AFM measurements which help explaining the corrosion process. The three dimensional AFM images represented in Figure (11).
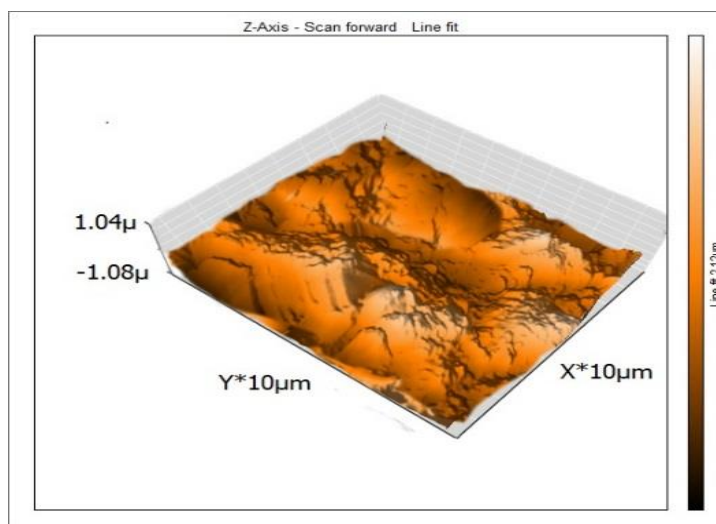
(a)Blank
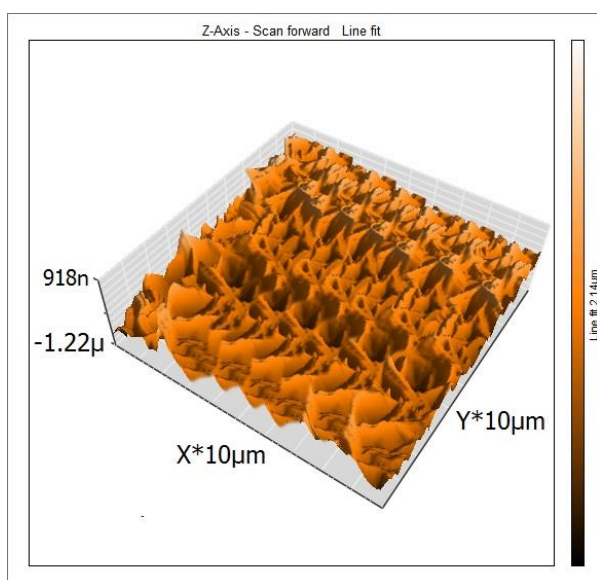
(b)Comp. (A)
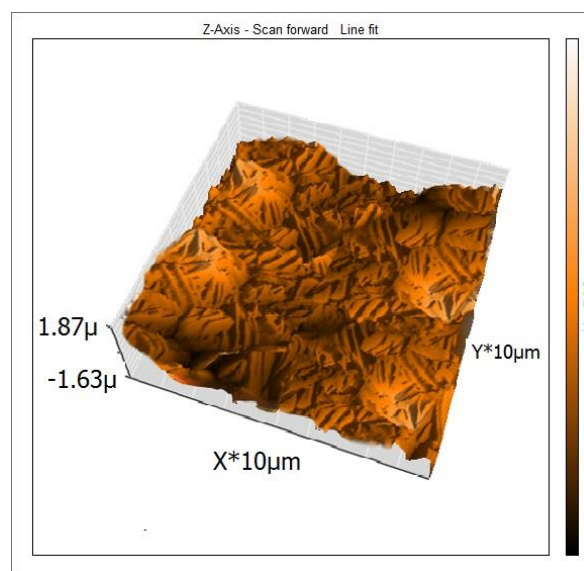
(c)Comp. (B)

Figure 11. (a) 3D AFM image of SS201 immersed 1.0M HCl for 1day, (b) 3D AFM image of SS 201 immersed in 1.0M HCl+21x10⁻⁶M of compound (A) for 1 day, (c) 3D AFM image of SS 201 immersed in 1.0M HCl+21x10⁻⁶M of compound (B) for 1 day

Table 9. AFM parameters of investigated hydrazine derivatives (A and B) at 25°C

Sample	Roughness average (Sa), nm
Blank	512
A	241
B	297

The roughness calculated from AFM image are summarized in Table (9). The values showed that the roughness increases with adding HCl due to the corrosion occurs on the SS 201 surface but decreased with adding the prepared [42].

3.9. (FT – IR) Analysis

Functional groups and characterizing covalent bonding knowledge had been identified by FT-IR which is an influential analytical device [43]. The finger print spectra of the compound (A) and the SS 201 surface after inundation in 1.0 M HCl + 21×10^{-6} to (A) for 180 min has achieved and compared to each other. (The same diagrams have achieved in the presence of the other compound (not shown). FTIR spectroscopy demonstrations, exciting features, for example power peak to noise ratio, great selectivity and little quantity of sample needed for the examination. Figure (12a and b) signify the IR spectrum of HD and the film produced on the SS 201. The FTIR of pure HD had shown Figure (12a) The -OH- frequency seems at 3407 cm^{-1}, the C=O seems at 1646 cm^{-1}, Aromatic ring seems at 744 cm^{-1}, the –SH frequency seems at 2101 cm^{-1}. The FTIR of the film coated on the SS 201 is displayed in Figure (12b). The -OH is stretching frequency moves from 3407 cm^{-1} to 3416 cm^{-1}. The –SH is stretching moves from 2101 cm^{-1} to 2093 cm^{-1}.
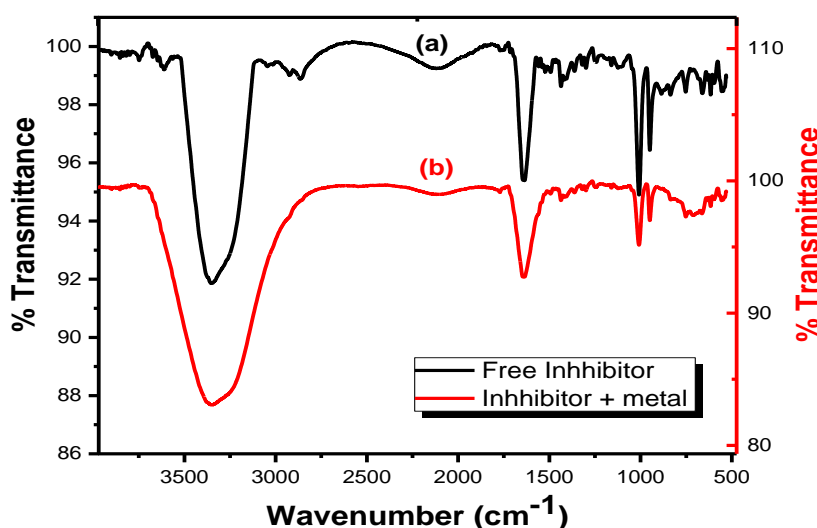

Figure 12. FTIR spectra of inhibitor (A) stock solution (black line) and a layer of compound (A) adsorbed on SS 201 surface (red)

3.10. Quantum Chemical Calculations

The inhibition behavior of (HD) for SS 201 corrosion in acidic solution can be discussed by quantum chemical studies using DFT method. The optimized geometry, frontier molecular orbital of HOMO, LUMO and the distribution of Mullikan charge of (HD) are plotted in Figure 13, respectively. It is shown that, the distributions of electron density were localized on HOMO and LUMO of inhibitors confirms the electron donating and accepting centers are possible in (HD) molecules. The detailed data of quantum chemical parameters for (HD) are calculated and listed in Table 10. According to the DFT theory, the inhibition efficiency of the investigated inhibitor for SS 201 corrosion in acidic solution is related to the energy of lowest unoccupied molecular orbital (E_{LUMO}), the energy of highest occupied molecular orbital (E_{HOMO}) and the energy gap ΔE ($\Delta E = E_{LUMO} - E_{HOMO}$) [44]. From the Table 10, it can be noted that, the higher E_{HOMO} values indicate that (compound

A) molecules can easily give electrons to the empty d-orbital of iron. But, the lower E_{LUMO} values show a higher electron accepting ability from the SS 201 metal. The smaller values of ΔE of compound (A) show the stability of formed complex on the SS 201 surface which determines the soft–soft interaction between the soft metal acid and the soft base inhibitor in the investigated system [45]. The Mullikan charge distributions of atoms for (compounds (A and B) obtained by DFT calculations are shown Figure 13. It is deduced that the more negative charge on heteroatoms, the more easily electrons donation and electrostatic attraction between the (HD) molecules and the SS 201 surface. From the quantum chemical analysis, it is found that, an agreement with the previously mentioned experimental data obtained by ML, PP, EFM, EIS tests.
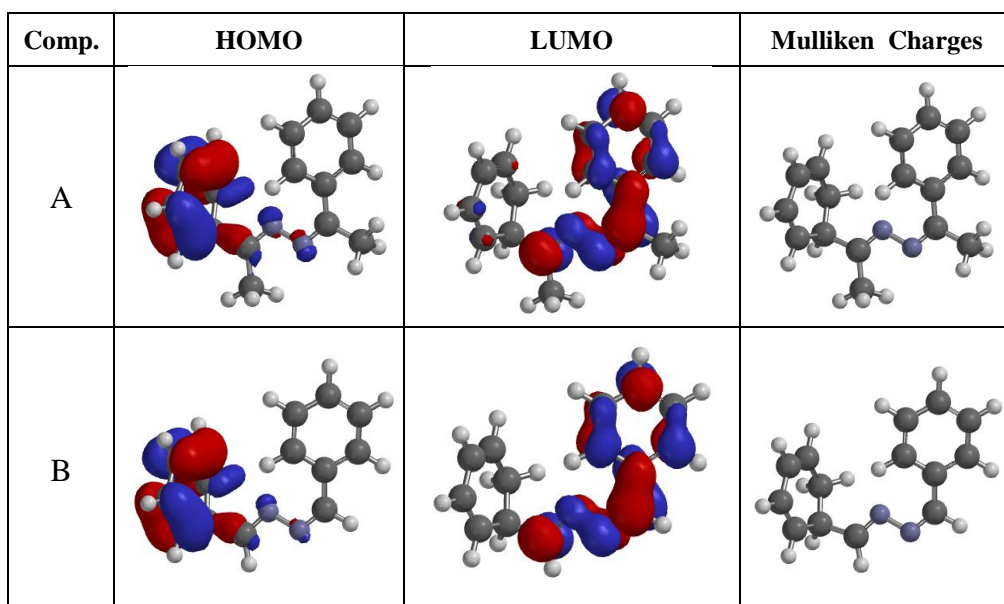
Comp.	HOMO	LUMO	Mulliken Charges
A			
B			

Figure 13. HOMO and LUMO electronic densities distributions of compounds (A and B) in liquid phase.

Table 10. Quantum chemical parameters for compounds (A and B) in liquid phase.

Parameter	Comp.(A)	Comp.(B)
E_{HOMO}(eV)	-8.93	-9.03
E_{LUMO} (eV)	-0.27	-0.51
ΔE (eV)	8.660	8.520
η(eV)	4.330	4.260
σ(eV^{-1})	0.231	0.235
Pi (eV)	-4.600	-4.770
χ (eV)	4.600	4.770
μ (debyes)	0.150	0.540

3.11 Mechanism of Inhibition

Four kinds of adsorption [46] may occur, including hydrazine derivatives at the interface of SS 201– solution: 1) Electrostatic attraction among the hydrazine molecules and SS 201; 2) Contact of unshared electron pairs in the hydrazine derivatives with the SS 201; 3) The interaction of metal π-electrons; 4) Summation of all the above. From the outcome data obtained from the various tests, corrosion hindrance of SS 201 in 1.0M HCl solutions by the hydrazine derivatives as designated from ML, PP, EFM and EIS tests were depended on the nature of the inhibitor and the dose. The sequence of IE is at: A > B. This order of the lowering in the IE of the tested compounds can be accounted for in terms of the polar influence [47]. A > B, this may be due to: the greater molecular size of (A) than (B) and the existence of the two donating groups (–CH$_3$) group in the molecule. It is generally considered that the surface of SS 201 had a positive charge in acid medium [48, 49], but it was establish that the surface of SS 201 carries negative charged in acid medium in the existence of hydrazine derivatives (because of the adsorption of Cl$^-$ ions on SS201) which allows the positively charged of hydrazine derivatives directly adsorb on the surface of SS 201 through electrostatic interaction.

The utilized HD as corrosion protection for SS 201 in 0.1 HCl was deliberated in terms of physical adsorption on the SS surface. This proved from the data of ΔG^o_{ads} (less than 20 kJ mol^{-1}) and also from the effect of temperature (%IE decreases by raising temperature). This molecule hydrazine derivatives will present in the protonated form, so it can adsorb directly on the negative surface of SS 201 [50] in acidic medium by electrostatic attraction as shown below
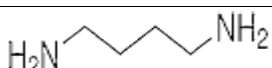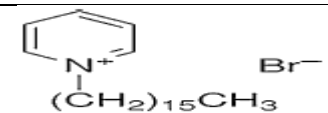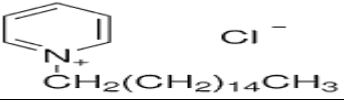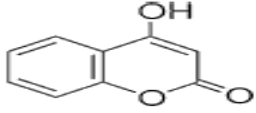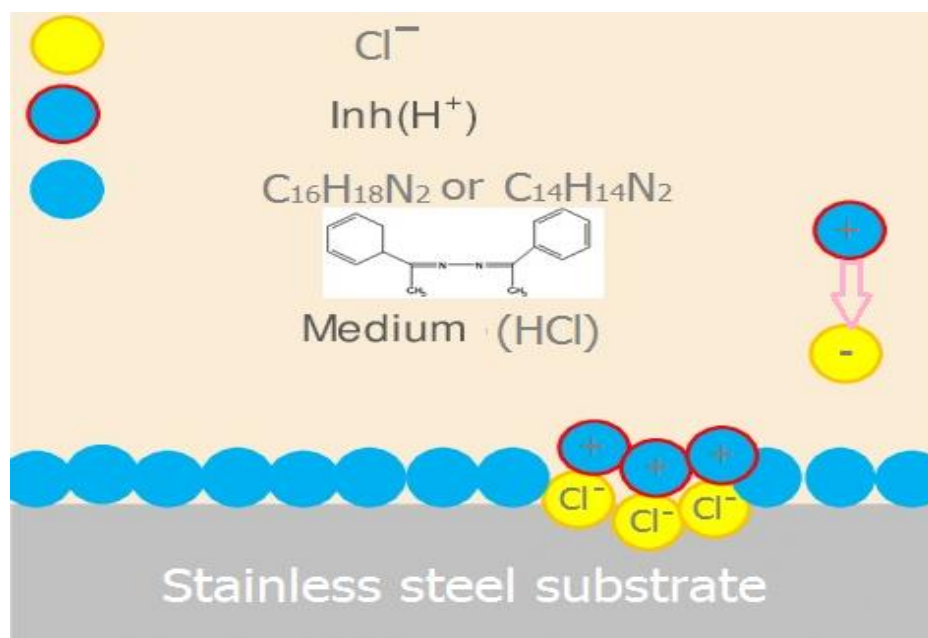

Table 11. gives a comparison of %IE with different investigated hydrazine derivatives. The present derivatives gives considerably significant corrosion %IE compared to other derivatives. Thus, the present hydrazine derivatives can be used as corrosion inhibitor with promising results.

Table 11. Performance comparison of some expired derivatives as corrosion inhibitors

Inhibitor	Structure	sample	IE%	References
1,4-Butanediamine	H_2N ⌒⌒⌒ NH_2	Stainless steel 304	51	51
1,8-Octanediamine	$H_2NCH_2(CH_2)_6CH_2NH_2$	Stainless steel 304	58	51
Cetylpyridinium bromide	N^+ Br^- $(CH_2)_{15}CH_3$	Carbon steel	87	52
Cetylpyridinium chloride	N^+ Cl^- $CH_2(CH_2)_{14}CH_3$	Carbon steel	81	52
4-Hydroxy coumarin	OH ... O O	Mild steel	61	53
organic compounds	present work	SS 201	86.3	This study

4. CONCLUSIONS

It was found that the percentage IE depends on the doses, and reached to higher data at higher dose of organic compounds, temperature and chemical structure of Organic compounds. The IE of the investigated organic compounds was in the order: A > B. The tested organic compounds behave as a mixed-kind corrosion protection in 1.0M HCl. The organic compounds acts among adsorption phenomenon and creation of barrier film due to lower in the C_{dl} with respect to the blank solution when added these organic compounds are. The adsorption of investigating organic compounds on SS 201 obeys Langmuir isotherm. The percentage IE of surfactants gotten from the ML, PP curves, EIS and EFM techniques are in best agreement.

References

1. D.C. France, *J Mater Eng. Perform*, 25(9) (2016) 3580.
2. S.L. Cohen, V.A. Brusic, F.B. Kaufman, G.S. Frankel, S. Motakef and B. Rush, *J. Vac. Sci. Technol. A.,* 8 (1990) 2417.
3. E.E. Ebenso, N.O. Eddy and A.O. Odiongenyi, *Port. Electrochim. Acta.*, 27 (2009) 13.
4. T. Peme, L.O. Olasunkanmi, I. Bahadur, A.S. Adekunle, M.M. Kabanda and E.E. Ebenso, *Molecules*, 20(9) (2015) 16004.
5. N.O. Eddy, H. Momoh-Yahaya and E.E. Oguzie, *Journal of advanced research*, **6**(2) (2015) 203.
6. N.M. Abdel-Hady, G.T. M. Dawoud, A. A. El-Hela and T.A. Morsy, *Journal of the Egyptian Society of Parasitology*, 41(3) (2011) 785.
7. S. Junaedi, A. Al-Amiery, A. Kadihum, A. Kadhum and A. Mohamad, *Int. J. Mol. Sci.,* 14(6) (2013) 1915.
8. A. Kadhum, A. Mohamad, L. Hammed, A. Al-Amiery, N. Hooi San and A. Musa, *Materials,* 7 (6) (2014) 4335.
9. A.S. Fouda, M. Abdallah, S.T. Atwa and M.M. Salem, *Modern Appl. Sci. Canda*, 4 (12) (2010) 41.

10. S.K. Rajappa and T.V. Venkatesha, *J. Electrochem. Soc. Ind.*, 51(2) (2002) 54.

11. M.T. Mohammed, *J. Electrochem. Soc. Ind.,* 551(2) (2002) 75.

12. D.A. Pisanenko and I.S. Pogrebova, *Zh. Prikl. Khim. J.,* 75(8) (2002) 1248.

13. L. Wang, X. Pu-Jian and L. Hui-Chun, *Corros. Sci.,* 45(4) (2003) 677.

14. M. Abdallah, *Corros. Sci.,* 45(12) (2003)2705

15. C.E. Kaan and O. Atakol, *Mater. Chem. Phys.,* 82(1) (2003) 188.

16. N. Mani, S. Venkatakrishna, L. Bahadur, *Transactions of the SAEST,* 38(2) (2003)67.

17. A.S. Fouda, F.M. El-Taweel, M. Elgamil, *Int. J. Electrochem. Sci.,* 12 (2017) 11397.

18. M. Abdallah1, M.M. Salem, B. A. AL Jahdaly, M.I. Awad, E. Helal and A.S. Fouda, *Int. J. Electrochem. Sci.,* 12 (2017) 4543.

19. M.A. Deyab, A.S. Fouda, M.M. Osmana and S. Abdel-Fattaha, *RSC Adv.,* 7 (2017) 45232.

20. A.S. Fouda, T. Fayed, M.A. Elmorsi, M. Elsayed, *J Bio Tribo Corros.,* 3(33) (2017) 1.

21. S.K. Shukla, M.A. Quraishi, E.E. Ebenso, *Int. J. Electrochem. Sci.*, 6 (2011) 2912.

22. X.H. Pang, W.J. Guo, W.H. Li, J.D. Xie, B.R. Hou, *Sci. China Ser. B-Chem.*, 51 (2008) 928.

23. R.W. Bosch, J. Hubrecht, W.F. Bogaerts, and B. C. Syrett, *Corrosion*, 57 (2001) 60.

24. S.S. Abdel–Rehim, K.F. Khaled and N.S. Abd–Elshafi, *Electrochim. Acta*, 51 (2006) 3269.

25. S.F. Mertens, C. Xhoffer, B.C. Decooman and E. Temmerman, *Corrosion*, 53 (1997) 381.

26. M. Lagrenée, B. Mernari, M. Bouanis, M. Traisnel and F. Bentiss, *Corros. Sci.*, 44 (2002) 573.

27. F. Bentiss, M. Lagrenée, and M. Traisnel, *Corrosion*, 56 (2000)733.

28. E. Kus and F. Mansfeld, *Corros. Sci.*, 48 (2006) 965.

29. D.Q. Zhang, Q.R. Cai, X.M. He, and G.S. Kim, *Mater. Chem. Phys.*, 114 (2009) 612.

30. G. Trabanelli, in "Corrosion Mechanisms" (Ed. F. Mansfeld) Marcel Dekker, New York, (1987) 119.

31. A.S. Fouda, A. Abd El-Aal and A.B. Kandil, *Desalination*, 201 (2006) 216.

32. A. Fiala, A. Chibani, A. Boulkamh and K. Djebbar, *Appl. Surf. Sci.*, 253 (2007) 9347.

33. W. Durnie, R.D. Marco, A. Jefferson and B. Kinsella, *J. Electrochem. Soc.*, 146 (1999) 1751.

34. M.K. Gomma and M.H. Wahdan, *Mater. Chem. Phys.*, 39 (1995) 209.

35. A.N. Frumkin, Advances in electrochemistry and electrochemical engineering, vol 3, chapter 5. Interscience Publisher Inc., New York, (1963).

36. F. Bensajjay, S. Alehyen, M. El Achouri, S. Kertit, *Anti-Corros. Meth. Mater*., 50 (2003) 402.

37. L. Tang, X. Li, Y. Si, G. Mu and G. Liu, *Mater. Chem. Phys.,* 95 (2006) 29.

38. G. Mu, X. Li and G. Liu, *Corros. Sci.*, 47 (2005) 1932.

39. B. Wang, M. Du, J. Zang and C.J, Gao, *Corros. Sci.*, 53 (2011) 353.

40. S. Rajendran, C. Thangavelu and G. Annamalai, *J. Chem. Pharm. Res.*, 4 (2012) 4836

41. A.S. Fouda, Y.M. Abdallah and D. Nabil, *IJIRSET,* 3 (2014) 12965

42. M. Abdallah, I. Zaafarany, S.O. Al-Karanee and A.A. Abd El-Fattah , *Arabian Journal of Chemistry,* 5 (2012) 225.

43. C.R. Jahromi, and K. Dehghanian, *Int. J. Current Res.,* 9(1) (2017) 44630.

44. N. Kumar Gupta, C. Verma, R. Salghi, H. Lgaz, A.K. Mukherjeea, M.A. Quraishi, New J. Chem., 41 (2017) 13114.

45. Y. Wang and Y. Zuo, *Corros. Sci.*, 118 (2017) 24.

46. D.P. Schweinsberg, A. Graeme and D.A. Steinert, *Corros. Sci.,* 19(4) (1988) 28

47. A.S. Fouda, M. Abdallah and Z. El-Badrawy, *Afri. J. Pure Appl. Chem.,* 5(8) (2011) 24.

48. G. Banerjee and S.N. Malhotra, *Corrosion,* 48 (1992) 10.

49. X. Li, X. Xie, S. Deng and G. Du, *Corros. Sci.,* 87(2014) 27.

50. H. Patmore, A. Jebreel, S. Uppal, C.H. Raine and P. Mc Whinney, *Am J Otolaryngol*, 31(5)(2010) 376

51. A.S. Fouda, H.A. Mostafa, G.Y. Elewady and M.A. El-hashemy, *Chem. Eng. Commun.,* 195 (2008) 934.

52. M.A.M. Menezes, M.L.M. Valle, J. Dweck, J.C. Queiroz Neto, *Brazil. J. Petrol. Gas,* 1(1) (2007)

6064

8.
53. S.R. Krishnamurthy, M.H.N. Parameswaran, *ISRN Corros.,* 2013(2013) 1.